Cellular/Molecular

Two Forms of Synaptic Plasticity with Distinct Dependence on Age, Experience, and NMDA Receptor Subtype in Rat Visual Cortex

Yumiko Yoshimura,[1] Tomohisa Ohmura,[2] and Yukio Komatsu[1]

[1]Department of Visual Neuroscience, Research Institute of Environmental Medicine, Nagoya University, Nagoya 464-8601, Japan, and [2]Department of Ophthalmology, Nagoya University School of Medicine, Nagoya 466-8550, Japan

In visual cortex, NMDA receptor (NMDAR) properties depend primarily on NR2A and NR2B subunits, and NR2 subunit composition changes with age and visual experience. We examined the roles of these NR2 subunits in activity-dependent long-term modification of synaptic responses, which were evoked in layer 2/3 cells by stimulation of layer 4 in rat visual cortical slices. We used theta-burst stimulation (TBS) of presynaptic fibers or low-frequency stimulation paired with postsynaptic depolarization, which has been commonly used to induce NMDAR-dependent long-term potentiation (LTP) in visual cortex. In pyramidal cells, however, TBS produced long-term depression (LTD) at inhibitory synapses rather than LTP at excitatory synapses. This was observed in association with LTP of extracellular field potentials that reflect postsynaptic potentials in a population of cells (field-LTP). This result is inconsistent with the previous view that field-LTP reflects LTP of excitatory connections. However, pairing stimulation produced LTP at excitatory synapses of pyramidal cells frequently during development but rarely in adulthood. In contrast, inhibitory LTD and field-LTP occurred similarly in both developing and mature cortex. Experiments using NR2B selective and NR2 subunit nonselective NMDAR antagonists demonstrated that NR2A- and NR2B-containing NMDARs contribute selectively to inhibitory LTD–field-LTP and excitatory LTP, respectively. In addition, we found that the developmental decline in the NR2B component was paralleled by a decline in the incidence of excitatory LTP, and these declines were both prevented by dark rearing. These results implicate NR2 subunit composition in the regulation of neocortical plasticity and demonstrate differential subunit regulation at inhibitory and excitatory connections.

Key words: **synaptic plasticity; long-term potentiation; long-term depression; NMDA receptor; NR2 subunit; visual cortex; development**

Introduction

Visual experience plays a crucial role in the maturation of mammalian visual cortical functions. Visual response properties are remarkably modifiable, depending on experience during a postnatal critical period, as documented by studies on the effects of monocular deprivation on ocular dominance preference (Wiesel, 1982; Frégnac and Imbert, 1984). The NMDA receptor (NMDAR) may be a key molecule involved in activity-dependent synaptic modification underlying this developmental process (Fox and Daw, 1993; Singer, 1995; Katz and Shatz, 1996). NMDARs are composed of both NR1 subunits, which are essential to channel function, and NR2 subunits, which convey distinct functional properties (Seeburg, 1993; Mori and Mishina, 1995). Of the four NR2 subunits, rodent cortex contains primarily NR2A and NR2B. Developmentally, NR2B subunits are already expressed at birth and increase to near a plateau level within the first 2 weeks, whereas NR2A subunits are first expressed in the second week and increase gradually in subsequent weeks (Watanabe et al., 1992; Monyer et al., 1994; Sheng et al., 1994). Therefore, the NR2A/NR2B ratio increases with maturation. In visual cortex, NR2 subunit alteration is postponed by visual deprivation (Nase et al., 1999; Quinlan et al., 1999), as is the termination of the critical period (Cynader and Mitchell, 1980; Fagiolini et al., 1994), suggesting that the NR2 subunit composition is involved in controlling that period.

If this is the case, the synaptic modifiability may depend on NR2 subunit composition in visual cortex. Several studies have reported that NMDAR-dependent long-term potentiation (LTP) of excitatory synaptic transmission is induced by high-frequency stimulation, tetanic and theta-burst stimulation (TBS) of presynaptic fibers, or low-frequency stimulation paired with postsynaptic depolarization in visual cortex, as in the hippocampus (Artola and Singer, 1987; Kimura et al., 1989; Kirkwood and Bear, 1994; Yoshimura and Tsumoto, 1994). Most neocortical studies, however, did not analyze EPSPs isolated from IPSPs. Some of the previously reported LTPs could reflect NMDAR-dependent long-term depression (LTD) at inhibitory synapses (Komatsu and Iwakiri, 1993), which allows excitatory inputs to produce

Received April 2, 2003; revised May 16, 2003; accepted May 23, 2003.

This study was supported by grants from the Japanese Ministry of Education, Culture, Science, Sports and Technology (12053228, 13480265, 13035018, and 13780652) and the Hori Information Science Promotion Foundation. We thank Dr. E. M. Callaway for critical reading of this manuscript.

Correspondence should be addressed to Dr. Yumiko Yoshimura, Department of Visual Neuroscience, Research Institute of Environmental Medicine, Nagoya University, Furo-cho, Chikusa-ku, Nagoya 464-8601, Japan. E-mail: yyumiko@riem.nagoya-u.ac.jp.

Copyright © 2003 Society for Neuroscience 0270-6474/03/236557-10$15.00/0

larger depolarizing responses. This could lead to the incorrect interpretation that LTP had occurred at excitatory synapses.

In this study, we therefore recorded isolated EPSPs and IPSPs and tested the roles of NR2 subunits in visual cortical synaptic plasticity. Experiments were conducted in layer 2/3, where the manipulation of visual inputs produces rapid plastic changes of response properties during the critical period (Trachtenberg et al., 2000) and some changes even in adults (Gilbert, 1998). In contrast to the previous view, we found that TBS produced LTD of IPSPs but not LTP of EPSPs, in association with LTP of extracellular field potentials reflecting postsynaptic potentials in a population of cells (field-LTP); however, pairing stimulation could produce LTP in excitatory connections. Pharmacological study demonstrated that NR2A- and NR2B-containing NMDARs contribute selectively to inhibitory LTD and excitatory LTP, respectively. The NR2B component and excitatory LTP incidence changed in parallel with age and visual experience, indicating that the NR2 subunit composition is involved in the regulation of visual cortical synaptic plasticity.

Materials and Methods

Experiments were conducted using Sprague Dawley rats at postnatal day (PD) 20–30, except for the age-dependence study. Some rats were reared in a completely dark room from birth to adulthood (PD 60–90). As described previously (Komatsu, 1994), coronal slices of primary visual cortex (400 μm thick) were prepared from rats under deep anesthesia with isoflurane and kept in normal artificial CSF (ACSF) containing (in mM): 126 NaCl, 3 KCl, 1.3 $MgSO_4$, 2.4 $CaCl_2$, 1.2 NaH_2PO_4, 26 $NaHCO_3$, and 10 glucose at 33°C. When 20 μM bicuculline methiodide (BMI) was added to ACSF to block $GABA_A$ receptor–mediated IPSPs, the ACSF contained a high concentration (4 mM) of $CaCl_2$ and $MgCl_2$ to avoid excess excitability. In this case, NaH_2PO_4 and $MgSO_4$ were omitted and NaCl concentration was reduced to compensate for ACSF osmolarity. To record EPSPs isolated from IPSPs in ACSF containing a normal concentration of divalent cations, inhibition was blocked locally. BMI was diffused from a glass pipette (tip diameter, ~10 μm) that was filled with ACSF containing 5 mM BMI and placed <100 μm from the recording electrode (see Fig. 2*D*). To block EPSP–EPSC completely, 40 μM 6,7-dinitroquinoxaline-2,3-dione (DNQX), a non-NMDAR antagonist, and 100 μM DL-2-amino-5-phosphonovaleric acid (DL-APV), an NMDAR antagonist, were added to ACSF. NMDAR EPSPs were analyzed in ACSF containing 20 μM BMI, 40 μM DNQX, and 400 μM D-serine, which reversed the depressive action of DNQX on the NMDAR glycine site. NMDAR EPSCs were analyzed in ACSF containing 20 μM BMI and 10 μM 2,3-dioxo-6-nitro-1,2,3,4-tetrahydrobenzo[f]quinoxaline-7-sulfonamide (NBQX), another non-NMDAR antagonist lacking action on the NMDAR glycine site.

Two pairs of bipolar stimulating tungsten electrodes were placed in layer 4, separated from each other by ~0.5 mm (see Fig. 1*A*). A surgical cut was imposed in layers 4/5 to ensure that separate groups of presynaptic fibers were activated. One electrode was used to test the effect of conditioning stimulation and the other served as a control. Test stimulation was applied alternately to the electrodes at intervals of 5 sec. We used two types of conditioning stimulation, which were five episodes of TBS (12 bursts at 5 Hz, each burst contained four pulses at 100 Hz) at 0.1 Hz, and low-frequency stimulation (100 pulses at 1 Hz) paired with postsynaptic depolarization (between −10 and 0 mV) using current injection through patch electrodes. In a part of the experiments, however, we used tetanic stimulation (50 Hz, 1 sec) repeated 10 times at 0.1 Hz and TBS paired with postsynaptic depolarization. Test stimulus intensity was adjusted to yield the subthreshold of EPSPs required to initiate action potentials when intracellular responses were recorded with sharp or patch electrodes and a roughly half-maximal response when only field potentials were recorded. The intensity of TBS and tetanic stimulation was adjusted to twice the test stimulus intensity. In some of the nonpyramidal cells, however, the intensity of TBS was increased to four times the test stimulus intensity, which produced almost maximal responses. When the effect of TBS on IPSCs was examined, the intensity was adjusted as in the case of EPSP studies. In experiments conducted in ACSF containing 0.5 μM BMI (see Fig. 2*A*), very weak test stimulation was used to evoke EPSPs without accompanying IPSPs. For this purpose, we selected cells in which the threshold intensity was lower for evoking EPSPs than it was for IPSPs, and test stimulation intensity could be set to a value 10–30% higher than the threshold, at which no indication of superposition of IPSPs on EPSPs was detected. The intensity of TBS was adjusted to the value that evoked the first response with a rising slope larger than 5 mV/msec. TBS and tetanic stimulation used in any of the present experiments produced orthodromic spikes in recorded cells. The amplitude of the TBS-evoked response was assessed by using the rising slope of the first intracellular response during TBS.

Extracellular field potentials were recorded with glass pipettes filled with saline containing 2% pontamine sky blue. Intracellular responses were recorded from layer 2/3 regular spiking cells except for an experiment in which we studied the effect of TBS on nonpyramidal cells. Postsynaptic responses were recorded with sharp or patch pipettes. The sharp pipettes contained 2 M K-methylsulfate (40–60 MΩ). We selected cells with a stable resting membrane potential (less than −55 mV) and monitored input resistance throughout the experiments by injecting hyperpolarizing current pulses. For whole-cell recording, patch pipettes (4–6 MΩ) were filled with a solution containing (in mM): 140 K-gluconate, 8 KCl, 2 NaCl, 0.2 EGTA, 10 HEPES, 3 MgATP, and 0.5 Na_2GTP, pH 7.2 with KOH. When NMDAR EPSCs were analyzed, a Cs^+-base internal solution containing 10 mM BAPTA was used to avoid possible Ca^{2+}-dependent response changes. We selected cells with a high seal resistance (>1 GΩ) and a series resistance <30 MΩ for analysis. In some experiments, layer 2/3 pyramidal and nonpyramidal cells were recorded under infrared differential interference contrast (IR-DIC) optics (BX50WI, Olympus). When recording under current-clamp mode, the experiments were conduced similarly to those with sharp electrodes. Under voltage-clamp mode, we continuously monitored series and input resistance by applying hyperpolarizing voltage steps and did not compensate for series resistance. We analyzed only monosynaptic EPSPs–EPSCs. Responses were considered monosynaptic when the onset latency was almost constant (<0.3 msec) while the rising slope changed substantially at different stimulation intensities and during high-frequency stimulation (Komatsu et al., 1991). In the experiments studying LTD of IPSCs in pyramidal cells, presynaptic inhibitory cells were stimulated focally with another patch pipette placed on the soma (see Fig. 4*A*). The focal stimulating electrode was placed between the recording pipette and the massive stimulating electrode, and the horizontal distance between these two stimulating electrodes was adjusted to <100 μm, unless stated otherwise, so that TBS activated the inhibitory synapses, which were tested by focal stimulation.

The laminar location of stimulating and recording electrodes was histologically identified as described previously (Komatsu, 1994). In some cases, 0.3% neurobiotin was included in patch electrodes to stain the recorded cells. After recording, slices were fixed and resectioned as described previously (Yoshimura et al., 2000). Sections were processed by a method using Cy3-conjugated streptavidin (Sun et al., 1998), and labeled neurons were imaged with a Zeiss LSM510 (Oberkochen, Germany) confocal microscope. Staining was conducted on 20 regular spiking cells in the pairing stimulation experiments ($n = 4$, PD 7–13; $n = 5$, PD 20–30; $n = 3$, PD 60–90; $n = 8$, dark reared) and also on an additional 32 regular spiking cells ($n = 5$, PD 7–13; $n = 15$, PD 20–30; $n = 12$, PD 60–90). All of these were identified as pyramidal cells in layer 2/3. Intracellular staining with neurobiotin also confirmed the identification of pyramidal ($n = 8$, PD 7–13; $n = 11$, PD 20–30; $n = 8$, PD 60–90) and nonpyramidal cells ($n = 14$, PD 20–30) under IR-DIC optics.

Data were expressed as mean ± SEM and Student's *t*, Welch's, or Mann–Whitney *U* test was applied. The drugs used were obtained from the following sources: D-APV, DL-APV, NBQX, and DNQX from Tocris (Bristol, UK); ifenprodil, Ro 25–6981, BMI, and Cy3-conjugated streptavidin from Sigma-RBI (St. Louis, MO); and neurobiotin from Vector Laboratories (Burlingame, CA).

Results

Postsynaptic responses evoked by layer 4 stimulation were recorded from layer 2/3 of visual cortical slices prepared from rats at PD 20–30 during the critical period (Fagiolini et al., 1994). As shown in Figure 1, TBS of layer 4 consistently produced field-LTP, which was blocked by D-APV, an NMDAR antagonist. This LTP is essentially identical to that reported previously (Kimura et al., 1989; Kirkwood and Bear, 1994).

Pairing stimulation but not TBS produces LTP at excitatory synapses

To test whether field-LTP reflects changes at excitatory synapses, monosynaptic EPSPs were recorded from regular spiking, presumably pyramidal cells (Connors and Gutnick, 1990; Mason and Larkman, 1990), using sharp electrodes together with field potentials (Fig. 1*A*). We used test stimulation producing EPSPs that were subthreshold for orthodromic spikes. In a preliminary study, a pharmacological blockade of EPSPs showed that such monosynaptic EPSPs were evoked occasionally without accompanying monosynaptic IPSPs. If TBS can induce LTP at excitatory synapses, LTP would occur in such cases too. TBS always produced field-LTP (>15% increase from the baseline level), but it produced LTP of intracellular postsynaptic responses only in approximately half of the cells (Fig. 1*B–D*). Blocking of EPSPs always uncovered monosynaptic IPSPs for pathways that showed intracellular LTP (Fig. 1*B*) but never for pathways that lacked intracellular LTP (Fig. 1*C*). However, no significant difference ($p > 0.9$) was found in the TBS-evoked response, assessed by the rising slope of the first intracellular response during TBS, resting membrane potential, or input resistance between the former (6.9 ± 1.2 mV/msec; -65 ± 3 mV; 49 ± 5 MΩ; $n = 5$) and the latter groups (7.4 ± 0.9 mV/msec; -68 ± 3 mV; 47 ± 6 MΩ; $n = 6$). Furthermore, there was no significant difference ($p > 0.8$) in the magnitude of field-LTP between the two groups (Fig. 1*D*). Thus, the TBS-induced modification in field potentials may reflect changes in IPSPs rather than EPSPs.

In some previous studies, $GABA_A$ receptor-mediated inhibition was partially blocked with a bath application of BMI to facilitate the induction of NMDAR-dependent LTP (Artola and Singer, 1987; Kimura et al., 1989). Thus, we also tested whether TBS induces LTP of EPSPs in such conditions. To record EPSPs isolated from IPSPs, we used very weak test stimulation and selected cells in which only EPSPs seemed to be evoked by that stimulation. The absence of IPSPs was confirmed by a pharmacological blockade of EPSPs at the end of the experiment. In the presence of BMI at 0.5 μM, which was the dose often used, TBS produced no changes in EPSPs (Fig. 2*A*). The rising slope of the first intracellular response during TBS (8.6 ± 1.0 mV/msec; $n = 8$) was larger than that demonstrated in the experiments shown in Figure 1, in which TBS always induced field-LTP in the normal ACSF. These results also suggested that TBS cannot easily induce LTP of EPSPs.

This possibility was further examined under a complete blockade of IPSPs, using the blind-patch whole-cell recording method. Because a bath application of $GABA_A$ receptor antagonists at high doses increases excitability extremely and hence makes it difficult to obtain stable test responses, experiments were conducted in ACSF containing a high concentration of $CaCl_2$ and $MgCl_2$. We confirmed that this divalent cation modification alone did not affect field-LTP substantially (Fig. 2*B*). Nonetheless, neither TBS nor tetanic stimulation induced any clear LTP of EPSPs under IPSP blockade (Fig. 2*C*,*E*). The rising slope of the first response during TBS was 9.1 ± 0.7 mV/msec ($n = 8$), which was larger than the values in the experiments shown in Figure 1. We also tested this issue in ACSF containing a normal concentration of divalent cations by blocking IPSPs locally with a glass pipette containing 5 mM BMI placed near the

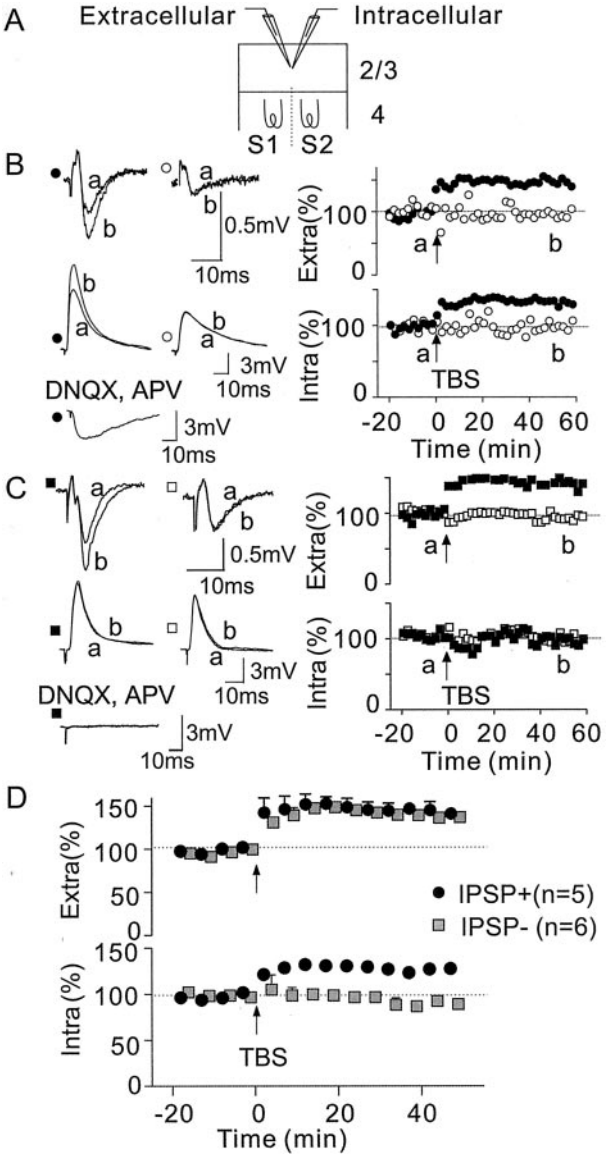

Figure 1. TBS produces LTP of intracellular postsynaptic potentials only in the presence of IPSPs. *A*, The arrangement of extracellular and intracellular recording electrodes and bipolar stimulating metal electrodes (S1 and S2). *B*, Example LTP of extracellular field potentials associated with LTP of intracellular postsynaptic responses. Top and middle traces show superimposed averages ($n = 5$) of extracellular and intracellular responses evoked by test stimulation for test (filled circles) and control pathways (open circles) before (*a*) and after (*b*) TBS, respectively. The intensity of TBS was adjusted to twice the test stimulus intensity. The average number of traces shown in the following figures was five or six, unless stated otherwise. The recorded time of the traces (*a*, *b*) is indicated in the graph on the right, where the amplitude of extracellular field potentials (top) and the initial slope of intracellular responses (bottom) (percentage of the mean baseline) are plotted against the time after TBS (arrow) for test (filled circles) and control (open circles) pathways. The bottom trace shows test pathway IPSPs recorded at membrane potentials of approximately −50 mV using a depolarizing current injection under EPSP blockade at the end of the experiments. *C*, Similar to *B*, but for field-LTP not associated with LTP of intracellular responses. IPSPs were not detected for the test pathway, although the membrane potential was depolarized to approximately −50 mV by a current injection. *D*, The amplitude of extracellular field potentials (top) and the initial slope of intracellular responses (bottom) (mean ± SEM) plotted against the time after TBS in cases with (circles; $n = 5$) and without IPSPs (squares; $n = 6$) for the test pathway.

recording electrode. TBS also failed to induce LTP of EPSPs (Fig. 2*D*,*E*), whereas the rising slope of the first response during TBS was 7.8 ± 0.5 mV/msec ($n = 10$). Taken together, these results suggest that high-frequency stimulation is usually unable to produce LTP at excitatory synapses, contrary to the previous view (Artola and Singer, 1987; Kimura et al., 1989; Kirkwood and Bear, 1994).

In contrast to TBS, pairing stimulation produced input-specific LTP of EPSPs (>20% increase from the baseline level) in more than half of the cells under IPSP blockade (Fig. 3*A*,*B*). However, no significant difference ($p > 0.2$) was found in the resting membrane potential or input resistance between the two groups of cells to which TBS (−69 ± 2 mV; 93 ± 12 MΩ; $n = 8$) or pairing stimulation (−72 ± 1 mV; 104 ± 7 MΩ; $n = 15$) was applied in ACSF containing 20 μM BMI. This LTP was NMDAR dependent because it was blocked by 100 μM DL-APV (Fig. 3*B*). TBS might produce a depolarization insufficient to induce LTP, because EPSPs usually undergo a transient depression caused by a reduced transmitter release during high-frequency stimulation in neocortical pyramidal cells, which is different from that of hippocampal pyramidal cells (Thomson and Deuchars, 1994; Castro-Alamancos and Connors, 1997). Thus, TBS was paired with postsynaptic depolarization. LTP was induced in some cells, but far less frequently compared with low-frequency pairing stimulation (Fig. 3*B*). Therefore, the ineffectiveness of TBS may be explained by an insufficient level of NMDAR activation, which is ascribable to both reduced transmitter release itself and a resultant insufficient postsynaptic depolarization.

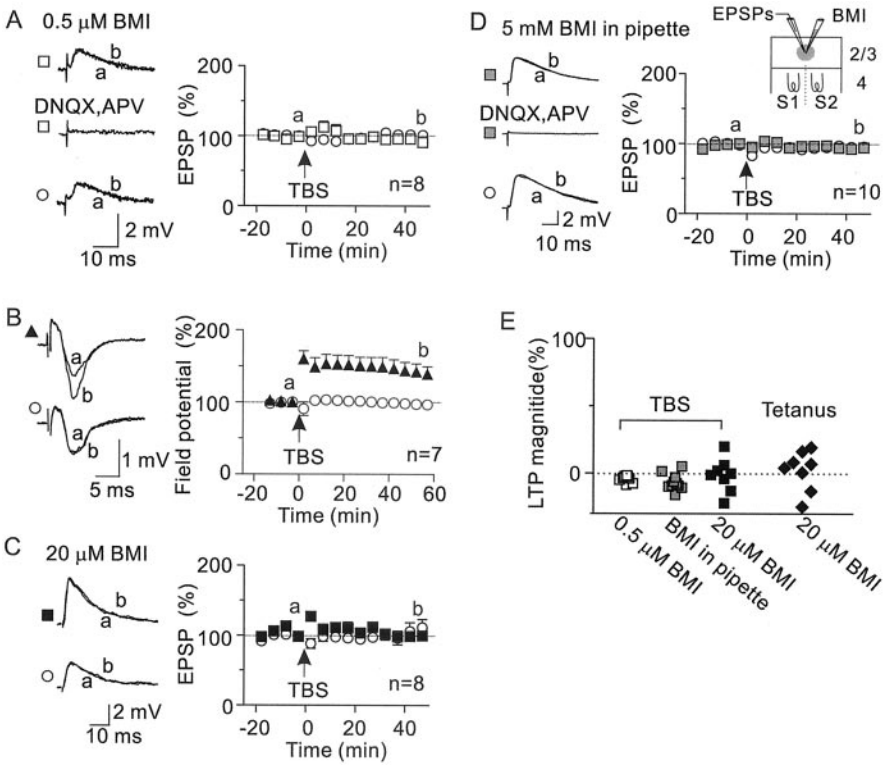

Figure 2. TBS fails to produce LTP of EPSPs under a blockade of IPSPs. *A*, Effects of TBS on EPSPs evoked by very weak test stimulation in ACSF containing 0.5 μM BMI. Traces show the superimposed average EPSPs evoked by test stimulation in a cell before (*a*) and after (*b*) TBS for test (squares) and control pathways (circles), respectively. The bottom trace for the test pathway shows responses recorded at a membrane potential of approximately −50 mV under a pharmacological blockade of EPSPs (DNQX, APV) at the end of the experiment, confirming the absence of IPSPs in test responses. The initial rising slope of EPSPs was plotted against the time after TBS for test (squares) and control (circles) pathways (average for 8 cells). *B*, Effects of TBS on field potentials in ACSF containing a high concentration of Ca^{2+} and Mg^{2+}. Traces show the superimposed average field potentials evoked by test stimulation before (*a*) and after (*b*) TBS for test (filled triangles) and control pathways (open circles), respectively. The amplitude of field potentials was plotted against the time after TBS for test (filled triangles) and control (open circles) pathways (average for 7 slices). *C*, Similar to *B*, but for EPSPs recorded with patch pipettes under conditions in which 20 μM BMI was added to ACSF containing a high concentration of Ca^{2+} and Mg^{2+}. Filled squares and open circles represent responses for test and control pathways, respectively. Time course shown is an average for eight cells. *D*, Similar to *A*, but IPSPs were blocked locally with a glass pipette containing 5 mM BMI that was placed near the recording patch pipette. Time course shown is an average for 10 cells. *E*, Summary of experiments conducted under a bath application of 0.5 μM BMI for TBS (open squares), under a local application of BMI for TBS (gray squares), and under a bath application of 20 μM BMI for TBS (filled squares) and tetanic stimulation (diamonds). Each symbol represents the magnitude of LTP in EPSPs of individual cells, assessed 40–45 min after conditioning stimulation. Postsynaptic responses were recorded with patch electrodes except for the experiment shown in *A*, during which they were recorded with sharp electrodes.

TBS produces LTD of IPSPs in pyramidal cells but not LTD of EPSPs in nonpyramidal cells

To test whether TBS instead induces LTD at inhibitory synapses, we conducted whole-cell recordings from visually identified pyramidal cells in normal ACSF and obtained isolated monosynaptic inhibitory responses by the focal stimulation of single inhibitory cells with another glass electrode (Fig. 4*A*). Because the amplitude of IPSP is small at resting membrane potentials and very sensitive to changes in membrane potential, we analyzed IPSCs recorded under voltage clamp at −40 mV. TBS was applied in current-clamp recording mode through the metal electrode placed in layer 4. This induced LTD of IPSCs (>20% decrease from the baseline level) in all of the tested cells ($n = 7$) (Fig. 4*B*). The slope of the plot between membrane potential and IPSC amplitude, reflecting IPSC conductance, decreased significantly after TBS ($p < 0.001$; $n = 4$) (Fig. 4*C*); however, there was no significant difference ($p > 0.2$) in the reversal potential of IPSC, input resistance, or series resistance before (−65 ± 0.3 mV; $n = 4$; 131 ± 10 MΩ, 13 ± 1 MΩ; $n = 7$) and after TBS (−65 ± 0.5 mV; 129 ± 10 MΩ, 13 ± 2 MΩ). A pharmacological EPSC blockade conducted at the end of the experiments did not affect isolated responses, confirming that focal stimulation elicited only monosynaptic IPSCs (Fig. 4*C*). In these experiments, the focal stimulating electrode was placed near the massive stimulating electrodes (horizontal distance <100 μm); however, when they were separated >300 μm horizontally and a surgical cut was made between them, no change was found in isolated IPSCs after TBS (103 ± 4% of the baseline level; $n = 4$), suggesting that LTD occurred selectively at inhibitory synapses that were activated during TBS.

We also tested whether TBS induces LTD of EPSPs in inhibitory cells, because such modifications may reduce the inhibition on pyramidal cells and hence contribute to field-LTP. IPSPs were blocked by either bath or local application of BMI. TBS never produced LTD in EPSPs recorded from visualized layer 2/3 nonpyramidal cells under either total (97.7 ± 3.2% of the baseline level at 45–50 min after TBS; $n = 7$) or local IPSP blockade

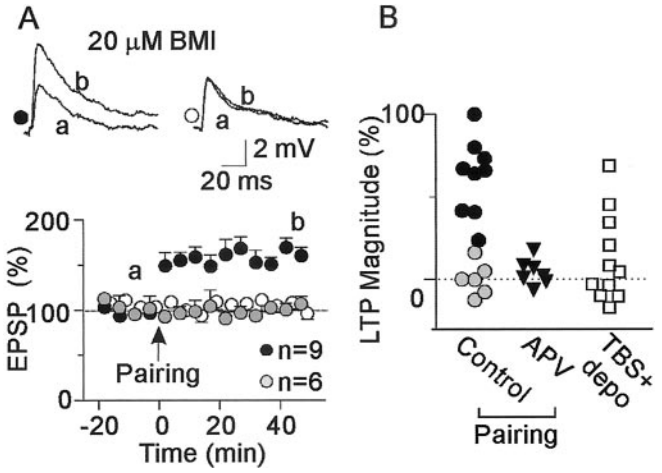

Figure 3. Pairing stimulation produces LTP of EPSPs. *A*, Similar to Figure 2*C* but for pairing stimulation. Gray and black circles represent an average for test pathway responses, where LTP did not ($n = 6$) and did occur ($n = 9$), respectively, and the open circles represent control pathway responses. *B*, Similar to Figure 2*E*, but for summary of experiments conducted under a bath application of 20 μM BMI for pairing stimulation without (circles) and with 100 μM DL-APV (triangles), and TBS paired with depolarization (squares).

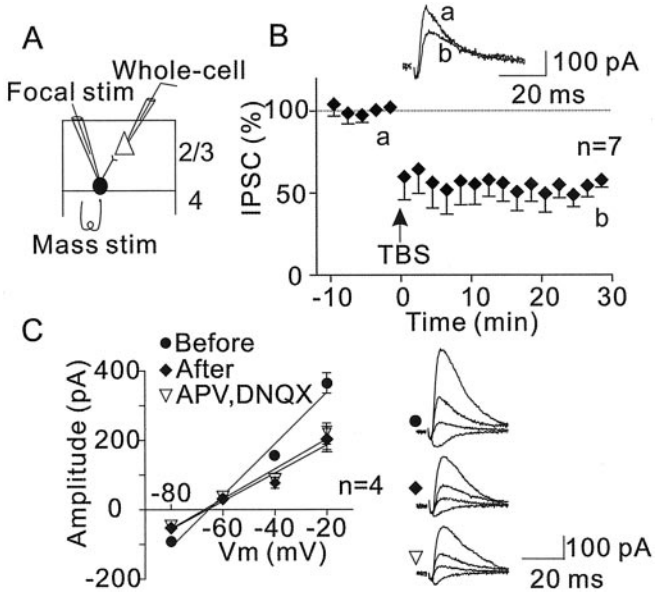

Figure 4. TBS induces LTD of IPSCs in pyramidal cells. *A*, The arrangement of massive stimulating electrodes for TBS and patch pipettes for focal stimulation and whole-cell recording. *B*, The amplitude of IPSCs plotted against the time after TBS (average for 7 cells). Traces show superimposed IPSCs in a pyramidal cell before (*a*) and after (*b*) TBS. *C*, Superimposed traces show test responses at −20, −40, −60, and −80 mV before (top) and after (middle) TBS and after EPSC blockade (bottom) in a cell. The left graph shows the *I–V* relationship for those responses (average for 4 cells).

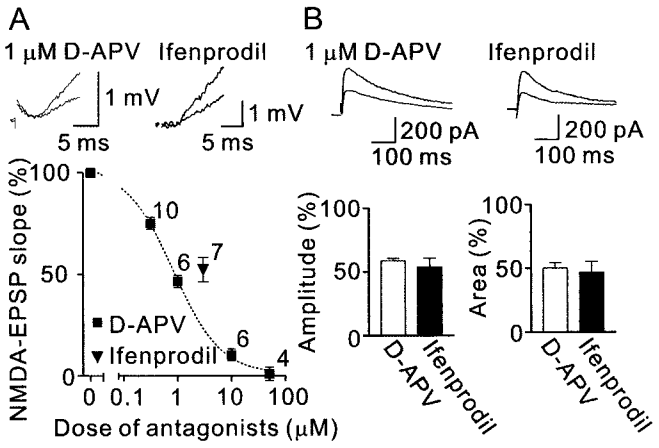

Figure 5. Effects of NMDAR antagonists on NMDAR EPSP–EPSC. *A*, Reduction of the rising slope of NMDAR EPSPs with D-APV (squares) and ifenprodil (triangle). Numbers attached to symbols indicate the number of tested cells. Traces show the superimposed average NMDAR EPSPs before and after application of 1 μM D-APV (left) or 3 μM ifenprodil (right). *B*, No significant difference ($p > 0.2$) was found in NMDAR EPSC reduction (percentage of the control value) assessed by the peak amplitude or the total area between 3 μM ifenprodil and 1 μM D-APV. The values were determined 30 min after starting the application of antagonists when the reduction of responses reached a steady level. NMDAR EPSCs were recorded from visualized pyramidal cells at +40 mV in the presence of NBQX and BMI. The number of cells was six for both ifenprodil and D-APV. Traces show the superimposed average ($n = 12$) NMDAR EPSCs in a cell before and after application of 1 μM D-APV (left) or 3 μM ifenprodil (right).

(106.5 ± 6.8%; $n = 7$). TBS was applied with similar ($n = 9$) or higher intensities ($n = 5$), compared with those used for pyramidal cells. The rising slope of the first response during TBS was 8.1 ± 2.1 ($n = 9$) and 15.8 ± 1.1 mV/msec ($n = 5$) for the former and the latter group of cells, respectively. Intracellular staining revealed smooth or sparsely spiny dendrites in these cells, which are characteristic of inhibitory interneurons (Connors and Gutnick, 1990). Thus, we suggest that LTD of inhibitory synaptic transmission in pyramidal cells is mainly responsible for field-LTP. Decreased inhibitory synaptic transmission may increase the postsynaptic depolarization resulting from excitatory inputs and the number of cells eliciting orthodromic spikes, which are both likely to contribute to the enlargement of field potentials. Consistent with this idea, it was reported that the amplitude of field potentials was increased by a bath application of BMI at a low dose (Bear et al., 1992).

Effects of NR2B-containing NMDAR antagonists on synaptic plasticity

To determine whether NR2A–NR2B subunits contribute differently to long-term modifications at excitatory and inhibitory synapses, we used ifenprodil, which noncompetitively blocks NR2B-containing NMDARs (Williams et al., 1993). Because no antagonist is known to selectively block NR2A-containing NMDARs, we also used D-APV, which blocks both but is more effective for NR2A- than for NR2B-containing NMDARs (Buller and Monaghan, 1997); results from D-APV were compared with the effects of ifenprodil. At 3 μM, ifenprodil blocks almost completely NR2B-containing NMDARs but does not affect those containing NR2A (Williams et al., 1993). We determined the dose of D-APV producing a blockade of NMDAR EPSPs comparable with 3 μM of ifenprodil, first using sharp electrodes instead of patch electrodes to avoid possible changes in the receptor function caused by intracellular washout. The rising slope of NMDAR EPSPs was reduced almost by half by 3 μM ifenprodil, and a comparable blockade ($p > 0.4$) was accomplished by 1 μM D-APV (Fig. 5*A*). At these doses, we confirmed that the antagonists produced almost the same degree of blockade in the peak amplitude and area of NMDAR EPSCs recorded from visualized pyramidal cells with patch electrodes (Fig. 5*B*).

Ifenprodil completely abolished LTP of EPSPs, but it did not affect LTD of IPSCs or field-LTP (Fig. 6). Because the blocker has some effects on voltage-gated channels and receptors other than NR2B-containing NMDARs (Chenard and Menniti, 1999), we also used a more potent antagonist (25-fold), Ro 25–6981, which

is likely to lack such side effects (Fischer et al., 1997; Mutel et al., 1998). The effect of Ro 25–6981 (0.3 μM) on excitatory LTP, field-LTP, and inhibitory LTD was indistinguishable ($p > 0.19$) from that of ifenprodil (Fig. 6*D*).

The effects of 1 μM D-APV were different from those of NR2B antagonists. Pairing stimulation produced excitatory LTP with a slightly but insignificantly ($p > 0.08$) reduced magnitude compared with the control solution, but it was significantly larger ($p < 0.02$) than in the presence of NR2B antagonists (Fig. 6*A*,*D*). APV significantly reduced both LTD of IPSCs and field-LTP at 1 μM ($p < 0.003$) and completely abolished them at 50 μM (Fig. 6*B–D*). These pharmacological profiles could not be explained by the mere difference in the total NMDAR activation level required for induction. Instead, they suggest that NR2A- and NR2B-containing NMDARs contribute selectively to the induction of LTD of IPSPs–field-LTP and LTP of EPSPs, respectively.

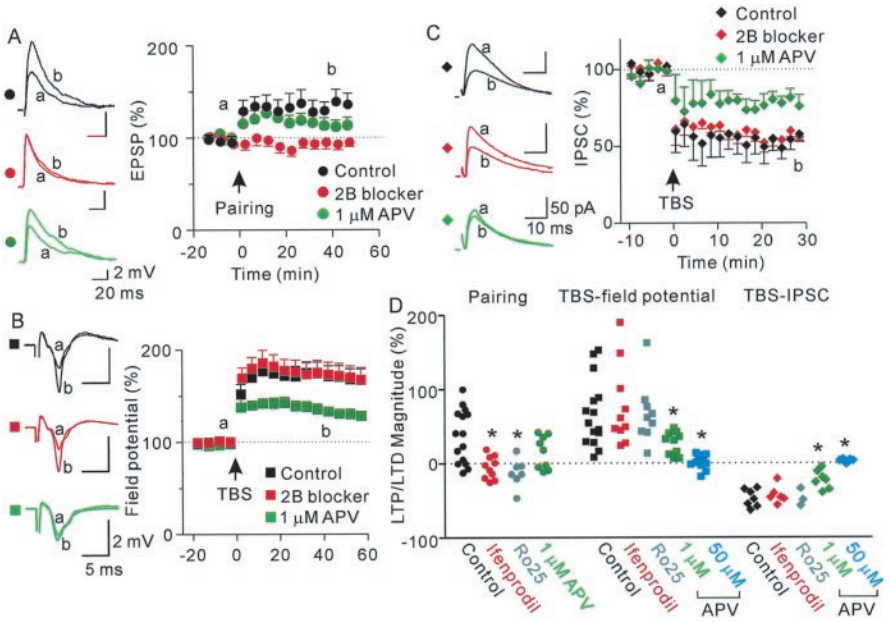

Figure 6. Effects of NMDAR antagonists on synaptic plasticity. *A*, Effects of NR2B antagonists and D-APV on LTP of EPSPs. Black, red, and green symbols plot the rising slope of test pathway EPSPs (mean ± SEM for all of the tested cells) against the time after pairing stimulation in control, NR2B antagonist (3 μM ifenprodil or 0.3 μM Ro 25–6981), and D-APV (1 μM) solution, respectively. The number of cells was 15 (control), 10 (ifenprodil), 7 (Ro 25–6981), and 9 (D-APV). Top, middle, and bottom traces show superimposed test pathway EPSPs before (*a*) and after (*b*) pairing stimulation in control, ifenprodil, and D-APV solution, respectively. *B*, Similar to *A*, but for field-LTP induced by TBS. The number of slices was 15 (control), 10 (ifenprodil), 9 (Ro 25–6981), and 10 (D-APV). *C*, Similar to *A*, but for LTD of IPSCs. The number of cells was 7 (control), 6 (ifenprodil), 3 (Ro 25–6981), and 7 (D-APV). *D*, The magnitude of excitatory LTP (circles), field-LTP (squares), and inhibitory LTD (diamonds) in control (filled black symbols) and in the presence of 3 μM ifenprodil (red), 0.3 μM Ro 25–6981 (gray), 1 μM D-APV(green), and 50 μM D-APV (blue). Values were determined 40–45, 55–60, and 25–30 min after conditioning stimulation for LTP of EPSPs, field-LTP, and LTD of IPSCs, respectively. Asterisks indicate values significantly different ($p < 0.05$) from control values.

Age and visual experience dependence of synaptic plasticity and NMDAR EPSC

These two forms of plasticity depending on different NR2 subunits showed different age dependence. Compared with the critical period (PD 20–30), LTP of EPSPs occurred more frequently at an early stage (PD 7–13), when the eyes have not yet opened, but never in adults (PD 60–90) (Fig. 7*A*). Regular-spiking cells were clearly identified in all age groups (Fig. 7*B*). The input resistance decreased significantly ($p < 0.0001$) from PD 7–13 (229 ± 15 MΩ; $n = 13$) to PD 20–30 (104 ± 7 MΩ; $n = 15$) but insignificantly ($p > 0.3$) from PD 20–30 to PD 60–90 (95 ± 6 MΩ; $n = 9$). The resting membrane potential was significantly depolarized ($p < 0.008$) at PD 7–13 (−64 ± 2 mV) compared with the later two stages (−72 ± 1 mV, PD 20–30; −72 ± 2 mV, PD 60–90), but no significant difference ($p > 0.8$) was found between the latter groups. Some of these cells were stained with neurobiotin and all were identified as pyramidal cells (Fig. 7*B*). Because the dendritic arbor size increased with age, the postsynaptic depolarization during pairing stimulation might have been insufficient to activate NMDARs located on dendrites far from the recording electrode in older rats. This is unlikely, however, because we confirmed that EPSPs were reversed around 0 mV (between −5 and +10 mV) in all age groups (Fig. 7*C*) ($n = 5$, PD 7–13; $n = 6$, PD 20–30; $n = 4$, PD 60–90).

When rats were reared in darkness from birth, pairing stimulation frequently produced LTP of EPSPs even in adults (Fig. 7*A*). The mean magnitude for all of the tested cells was the same as in normal rats at PD 20–30 (Fig. 7*A*). This result further excludes the possibility that the inability to produce LTP in normal adults was caused by poor recording quality, because no significant difference ($p > 0.2$) was found in the resting membrane potential, input resistance, or series resistance between normal (−72 ± 2 mV; 95 ± 6 MΩ, 21 ± 2 MΩ; $n = 9$) and dark-reared adults (−75 ± 2 mV; 90 ± 7 MΩ, 22 ± 3 MΩ; $n = 8$).

In contrast with LTP of EPSPs, LTD of IPSCs and field-LTP were both consistently produced by TBS in the critical period and adulthood (Fig. 8*A*,*B*), consistent with the previous report for field-LTP (Kirkwood et al., 1995). At the early stage (PD 13–15 for IPSCs, PD 11–13 for field potentials), these TBS-induced modifications occurred less frequently, and at a smaller magnitude, compared with the later two stages (Fig. 8*A*,*B*). The effect of dark rearing on field-LTP was also quite different from the effect on LTP of EPSPs (Fig. 8*B*). No difference was found in field-LTP between normal and dark-reared adults, as reported previously (Kirkwood et al., 1995).

The NR2B component of NMDAR EPSCs, assessed by ifenprodil sensitivity (Fig. 9*A*), declined with age in a close correlation with the developmental change in LTP of EPSPs (compare Figs. 9*B*, 7*A*). The value decreased significantly ($p < 0.05$), both from PD 7–13 to PD 20–30 and from PD 20–30 to PD 60–90. In addition, the component was significantly larger ($p < 0.01$) in dark-reared rats, compared with normal adults (Fig. 9*B*), as was LTP production. These results suggest that the change in the NR2B component is an important factor in the regulation of the capability of LTP. It was reported that age- and experience-dependent changes in the NR2B component estimated by ifenprodil were consistent with those estimated biochemically with antibodies for NR2 subunits in visual cortex (Quinlan et al., 1999).

A developmental decline in NMDAR EPSC decay was reported for various synapses (Hestrin, 1992; Crair and Malenka, 1995), including those in layer 4 cells of visual cortex where dark rearing prevented the decline (Carmignoto and Vicini, 1992). Because the duration of NMDAR EPSC may be an important

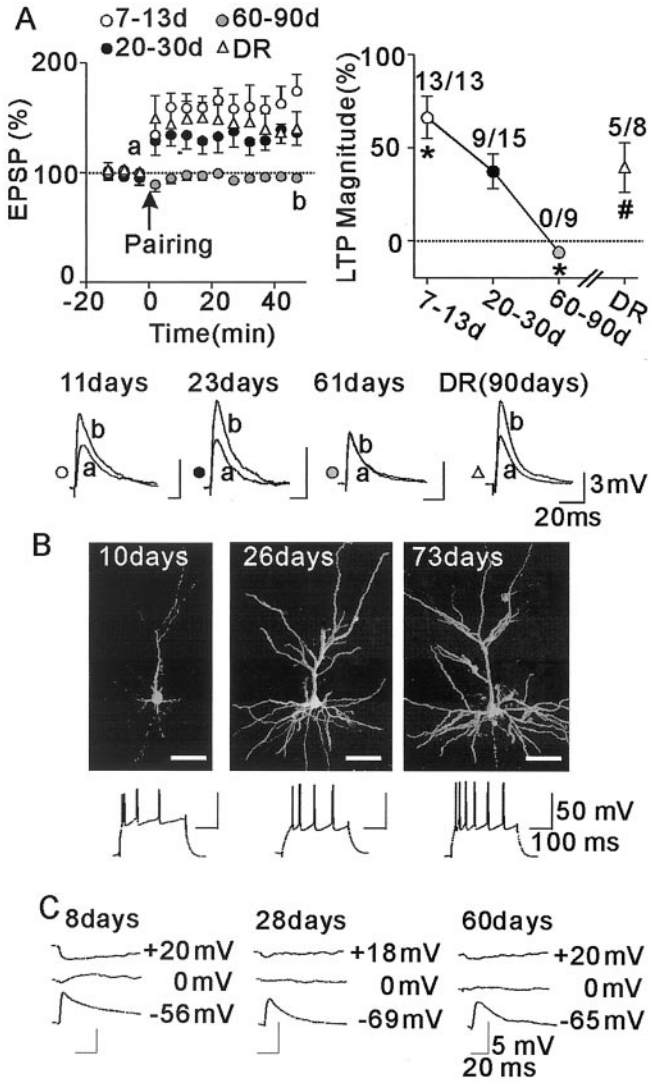

Figure 7. Age- and visual experience-dependent changes in excitatory LTP. *A*, The left graph plots the initial slope of test pathway EPSPs (mean ± SEM for all of the tested cells) against the time after pairing stimulation for different age groups (open circles, PD 7–13, $n = 13$; filled circles, PD 20–30, $n = 15$; gray circles, PD 60–90, $n = 9$) and dark-reared adults (triangles, $n = 8$). The right graph plots the magnitude (mean ± SEM) of excitatory LTP against postnatal days (average for all of the tested cells) and, in addition, values for dark-reared adults (DR). Values were determined as explained in the legend of Figure 6 *D*. The numbers on the symbols indicate the number of cases tested (denominator) and those that showed LTP (numerator). Asterisks indicate values significantly different ($p < 0.05$) from those at PD 20–30. The # symbol indicates that values for dark-reared rats were significantly different from those for normal adults. Bottom traces show superimposed test pathway EPSPs before (*a*) and after (*b*) pairing stimulation in cells sampled from rats at PD 11 (open circle), PD 23 (filled circle), and PD 61 (gray circle) and dark-reared adult (triangle). *B*, Examples of regular-spiking cells at PD 10, 26, and 73, which were identified as pyramidal cells by neurobiotin staining (confocal images for Cy3). Scale bar, 50 μm. Action potentials were initiated by an injection of 0.3 (left and center) and 0.5 nA depolarizing currents (right). *C*, EPSPs reversed around 0 mV by current injection in cells at PD 8, 28, and 60.

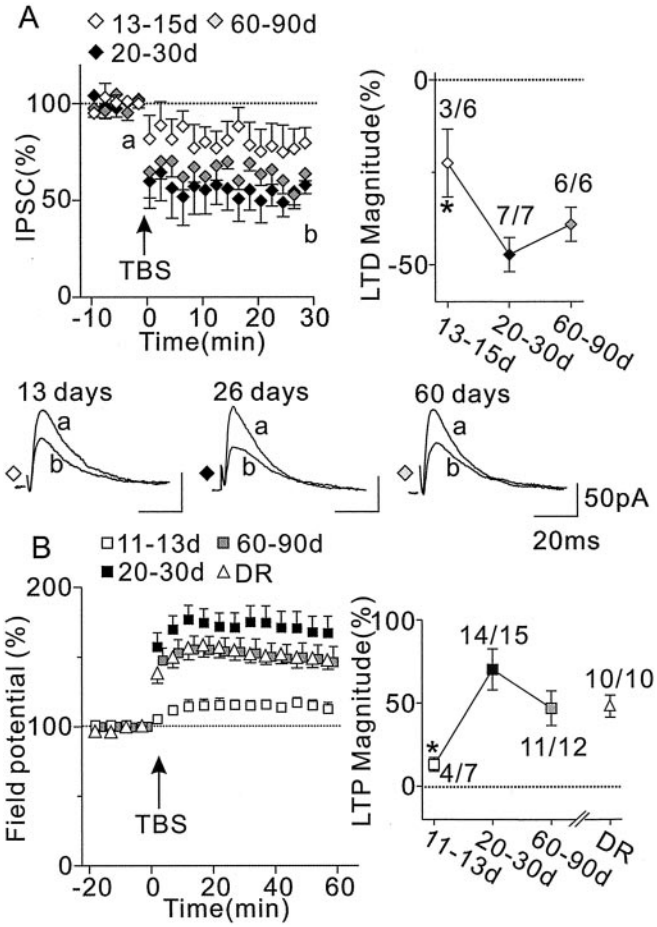

Figure 8. Age- and visual experience-dependent changes in TBS-induced synaptic plasticity. Time course (left graph) and magnitude (right graph) of inhibitory LTD (*A*) and field-LTP (*B*) are shown similarly to Figure 7*A*. In the right graph of *A* and *B*, values were determined as explained in the legend of Figure 6 *D*, and the numbers on the symbols indicate the number of cases tested (denominator) and those that showed inhibitory LTD or field-LTP (numerator). Asterisks indicate values significantly different ($p < 0.05$) from those at PD 20–30.

factor in determining the capability to produce plastic changes, we also analyzed NMDAR EPSC decay, which was well fit with a double exponential curve, as described previously (Carmignoto and Vicini, 1992). The decay time course was assessed by a time constant derived from the fast and slow components, weighted depending on amplitude (Philpot et al., 2001; Lu et al., 2001). The time constant decreased significantly ($p < 0.007$) from PD 7–13 to PD 20–30 but insignificantly ($p > 0.3$) from PD 20–30 to PD 60–90 (Fig. 9*C*). We found no significant difference ($p > 0.4$) in the value between normal and dark-reared adults (Fig. 9*C*), which was different from the result reported for layer 4 synapses of visual cortex (Carmignoto and Vicini, 1992). These results suggest that changes in the NR2B component rather than the decay time of NMDAR EPSC underlie the age- and experience-dependent changes in excitatory LTP.

Discussion

The present study demonstrated that TBS produced LTD at inhibitory synapses but not LTP at excitatory synapses in layer 2/3 pyramidal cells, whereas pairing stimulation produced the latter modification (Table 1). Inhibitory LTD occurred in both developing and mature cortex, whereas excitatory LTP occurred only during development, and dark rearing prevented this developmental decline. Pharmacological experiments suggest that NR2A- and NR2B-containing NMDARs contribute selectively to inhibitory LTD and excitatory LTP induction, respectively. An intimate relationship between the NR2B component and excitatory LTP production was suggested by their parallel changes with age and visual deprivation.

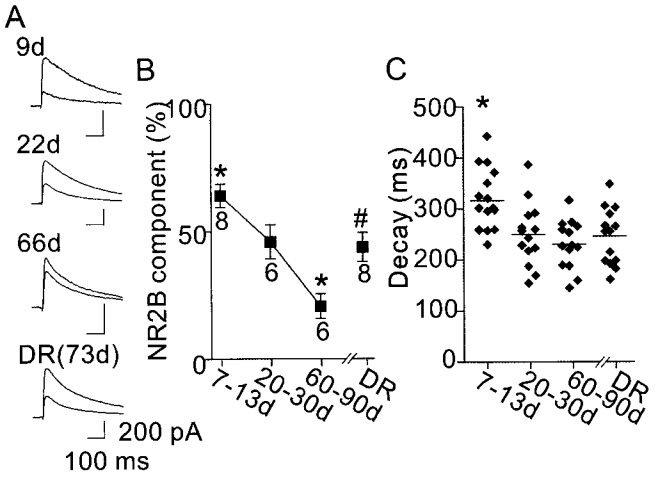

Figure 9. Age- and visual experience-dependent changes in NMDAR EPSC. *A*, Typical examples of NMDAR EPSCs recorded from visualized pyramidal cells at +40 mV. Average ($n = 12$) traces before and after the application of 3 μM ifenprodil are shown superimposed. The numbers on the traces indicate the age of the rat. DR indicates dark-reared rats. *B*, NR2B components assessed from the ifenprodil-induced reduction in NMDAR EPSC peak amplitude. The numbers on the symbols indicate the number of tested cells. *C*, Scatter plot of the weighted decay time constant for NMDAR EPSCs. The horizontal bar indicates mean values. In both *B* and *C*, the asterisks indicate values significantly different ($p < 0.05$) from those at PD 20–30. The # symbol indicates that values for dark-reared rats were significantly different from those for normal adults.

Table 1. Properties of NMDAR-dependent plasticity

	Excitatory LTP	Inhibitory LTD	Field-LTP
Conditioning stimulation	Pairing	TBS	TBS
NR2 subunit	2B	2A	2A
Age and experience Dependence	+	−	−

Ineffectiveness of TBS to induce LTP at excitatory synapses

High-frequency stimulation effectively produced NMDAR-dependent LTP of intracellularly and extracellularly recorded postsynaptic responses in visual cortex (Artola and Singer, 1987; Kimura et al., 1989; Kirkwood and Bear, 1994). Therefore it was concluded that high-frequency stimulation produces LTP at excitatory synapses, as in CA1 pyramidal cells where it is established. In CA1 pyramidal cells, high-frequency stimulation also produces NMDAR-dependent LTD at inhibitory synapses (Stelzer et al., 1987), which increases the capability of EPSPs to elicit spikes. This change is reflected in the relationship between the amplitude of population EPSPs and spikes in field potentials before and after high-frequency stimulation, revealed using various test stimulation intensities (Lu et al., 2000). In neocortex, however, EPSP and spike components of field potentials are not clearly separated, making it difficult to know which form of modification is produced. Thus we addressed this issue by analyzing isolated excitatory and inhibitory responses and demonstrated that TBS produced only inhibitory LTD, in contrast to the previous view. Thus it may be necessary to reconsider cautiously previous studies on synaptic plasticity using extracellular recording and high-frequency stimulation in neocortex.

This regional difference in the effect of high-frequency stimulation may be ascribed, at least partly, to the difference in frequency-dependent modification of EPSPs. Unlike CA1 pyramidal cells, EPSPs are depressed during high-frequency stimulation in neocortical pyramidal cells, and this depression is attributed to a reduction in transmitter release (Thomson and Deuchars, 1994; Castro-Alamancos and Connors, 1997). Excitatory LTP occurred far more frequently when postsynaptic depolarization was paired with presynaptic stimulation at low than at high frequency, despite fewer total stimuli with low-frequency (100 pulses) than high-frequency stimulation (240 pulses). Therefore, it is likely that low-frequency stimulation can more effectively activate NMDARs and hence induce excitatory LTP in layer 2/3 pyramidal cells, in such a condition that postsynaptic cells fire in association with presynaptic spikes (Feldman, 2000). On the other hand, TBS consistently produced inhibitory LTD, suggesting that inhibitory LTD requires NMDAR activation and a resultant intracellular Ca^{2+} elevation both at a level considerably lower than does excitatory LTP in visual cortex.

Differential contribution of NR2 subunits to synaptic plasticity

NMDARs seem to be composed mainly of three subunit combinations, NR1/NR2A, NR1/NR2B and NR1/NR2A/NR2B, in cerebral cortex (Sheng et al., 1994; Luo et al., 1997; Vicini et al., 1998; Tovar and Westbrook, 1999). Ifenprodil blocks the NR1/NR2B-type NMDARs but seems only weakly effective for NR1/NR2A- or NR1/NR2A/NR2B-type NMDARs (Cull-Candy et al., 2001). Thus, it is likely that NR2A and NR2B components, discriminated by ifenprodil, represent the NR1/NR2A- and NR1/NR2A/NR2B-type and NR1/NR2B-type NMDARs, respectively. The differential contribution of NR2A and NR2B components to inhibitory LTD and excitatory LTP might be explained merely by the difference in the intracellular Ca^{2+} level required for these modifications. Because NMDAR EPSCs decay faster when NMDARs contain more NR2A than NR2B subunits (Flint et al., 1997; Vicini et al., 1998), those containing more of the former may allow less Ca^{2+} entry and hence only the production of inhibitory LTD. However, this explanation is unlikely, because two forms of modifications were affected very differently by ifenprodil and D-APV using doses at which both antagonists reduced NMDAR EPSCs by approximately half. In addition, age- and experience-dependent changes in NMDAR EPSC decay were clearly different from those in the NR2B component and excitatory LTP production. Such dissociated developmental change was also found between the NR2B component and NMDAR EPSC decay at thalamocortical synapses of barrel cortex (Barth and Malenka, 2001), and NMDAR EPSC decay can be regulated by mechanisms other than NR2 subunit alteration (Shi et al., 2000).

A more plausible explanation for the differential contribution of NR2 subunits is suggested by a study using gene-targeted mice expressing NR2 subunits lacking the intracellular C-terminal domain (Sprengel et al., 1998). The mice expressing any of the truncated NR2 subunits showed functional impairments similar to those lacking that subunit totally, although Ca^{2+} entry through truncated NR2 subunit-containing NMDARs was normal. Because NMDAR activation may produce a high level of intracellular Ca^{2+} elevation mostly in the vicinity of the receptors (Regehr and Tank, 1994), NMDARs containing each type of NR2 subunit could activate separate downstream signal transduction molecules, leading to different cellular responses, via the physical link made by a specific interaction of these molecules and the C-terminal domain of each NR2 subunit (Husi et al., 2000). In CA1 pyramidal cells, high-frequency activation of excitatory synapses produces homosynaptic LTP at excitatory synapses through the activation of protein kinases (Bliss and Collingridge, 1993; Malenka and Nicoll, 1999) but heterosynaptic LTD at in-

hibitory synapses through the activation of protein phosphatases (Lu et al., 2000). Thus in layer 2/3 pyramidal cells, NR2A and NR2B subunits might contribute to the induction of these two forms of modification, respectively, through their selective linkage to different downstream molecules. Together with NMDAR activation, the activation of inhibitory synapses may be necessary for the induction of inhibitory LTD, because LTD seemed to occur only at inhibitory synapses activated by TBS, as was demonstrated for NMDAR-dependent LTD of GABAergic synaptic transmission in neonatal CA3 pyramidal cells (Caillard et al., 1999). When a direct postsynaptic depolarization produces postsynaptic Ca^{2+} entry through voltage-gated Ca^{2+} channels, inhibitory synapses undergo a transient depression called depolarization-induced suppression of inhibition in cerebellar Purkinje cells and hippocampal pyramidal cells (Llano et al., 1991; Pitler and Alger, 1992; Maejima et al., 2001). In contrast to inhibitory LTD, it is unlikely that this transient depression requires the activation of inhibitory synapses for induction.

LTP at thalamocortical synapses in barrel cortex is restricted to the first postnatal week and blocked by ifenprodil (Crair and Malenka, 1995; Lu et al., 2001). Developmental changes in that LTP production paralleled NR2B component reduction (Barth and Malenka, 2001), as shown here in layer 2/3 synapses, suggesting that alteration in NR2 subunit composition contributes to the determination of the critical period of LTP in sensory cortex. Furthermore, the present study demonstrated that dark rearing maintained high levels of LTP production and NR2B components. However, it was reported that in NR2A-lacking mutant mice, the critical period for LTP production at thalamocortical synapses ended at the same time as in wild-type mice, despite the maintenance of a high NR2B level beyond that period (Lu et al., 2001). Therefore, it is likely that NR2B components are necessary for LTP induction at excitatory synapses of sensory cortex, but it is not the sole molecule determining the ability to produce LTP. Multiple steps of LTP molecular mechanisms may be regulated developmentally and by experience.

Functional roles of two forms of synaptic plasticity

The two NMDAR-dependent modifications shown here may play different functional roles. Although both excitatory LTP and inhibitory LTD cause excitatory inputs to produce larger outputs, the latter may affect the input–output relationship in a more generalized manner, depending on the subcellular location of modified synapses. The difference in age dependence suggests that excitatory LTP contributes to experience-dependent refinement of developing cortical circuits, whereas inhibitory LTD contributes to plastic changes occurring even in mature cortex (Gilbert, 1998).

The susceptibility of ocular dominance preference to monocular deprivation in rat visual cortex is small around the time of eye opening, peaks around 4 weeks, and disappears in adults (Fagiolini et al., 1994). The decline of ocular dominance plasticity coincides well with the later developmental phase of excitatory LTP. Furthermore, when considered together, the previous studies (Cynader and Mitchell, 1980; Fagiolini et al., 1994) and present findings indicate that dark rearing similarly delays both processes, supporting the hypothesis that this LTP contributes to ocular dominance plasticity. However, a disagreement in the initial phase is evident, because LTP incidence was highest before eye opening. The NR2B component also decreased after eye opening in rats, as shown here, and in ferrets (Roberts and Ramoa, 1999). Thus one may argue that NR2B-dependent LTP is not directly involved in ocular dominance plasticity; however, we could not rule out the possibility that this LTP contributes to spontaneous activity as well as visual input-dependent plasticity. Spontaneous activity of retinal ganglion cells occurring before eye opening is thought to be indispensable for the segregation of inputs to cortical cells from two eyes (Katz and Shatz, 1996).

It has been suggested that TBS-induced field-LTP could be the basis of ocular dominance plasticity (Kirkwood et al., 1995). Such LTP in layer 2/3 exhibited age- and experience-dependent changes in parallel with ocular dominance plasticity when stimulation was applied to white matter but not layer 4 (Kirkwood et al., 1995). These authors proposed that the maturation of cortical inhibition is responsible for the changes in white matter stimulation-induced field-LTP and ocular dominance plasticity. Indeed, experimental modulation of GABAergic inhibition affected the critical period of ocular dominance plasticity and age-dependent decline of field-LTP (Hensch et al., 1998a; Huang et al., 1999). However, experiments using mutant mice lacking protein kinases demonstrated an inconsistent relationship between field-LTP and ocular dominance plasticity (Gordon et al., 1996; Kirkwood et al., 1997; Hensch et al., 1998b). The present finding of two forms of NMDAR-dependent synaptic plasticity, which can be distinguished pharmacologically, may contribute to the clarification of unresolved synaptic mechanisms underlying the experience-dependent development of visual cortex.

References

Artola A, Singer W (1987) Long-term potentiation and NMDA receptors in rat visual cortex. Nature 330:649–652.

Barth AL, Malenka RC (2001) NMDAR EPSC kinetics do not regulate the critical period for LTP at thalamocortical synapses. Nat Neurosci 4:235–236.

Bear MF, Press WA, Connors BW (1992) Long-term potentiation in slices of kitten visual cortex and the effects of NMDA receptor blockade. J Neurophysiol 67:841–851.

Bliss TVP, Collingridge GL (1993) A synaptic model of memory: long-term potentiation in the hippocampus. Nature 361:31–39.

Buller AL, Monaghan DT (1997) Pharmacological heterogeneity of NMDA receptors: characterization of NR1a/NR2D heteromers expressed in *Xenopus* oocytes. Eur J Pharmacol 320:87–94.

Caillard O, Ben-Ari Y, Gaïarsa J-L (1999) Mechanism of induction and expression of long-term depression at GABAergic synapses in the neonatal rat hippocampus. J Neurosci 19:7568–7577.

Carmignoto G, Vicini S (1992) Activity-dependent decrease in NMDA receptor responses during development of the visual cortex. Science 258:1007–1011.

Castro-Alamancos MA, Connors BW (1997) Distinct forms of short-term plasticity at excitatory synapses of hippocampus and neocortex. Proc Natl Acad Sci USA 94:4161–4166.

Chenard BL, Menniti FS (1999) Antagonists selective for NMDA receptors containing NR2B subunit. Curr Pharm Des 5:381–404.

Connors BW, Gutnick MJ (1990) Intrinsic firing patterns of diverse neocortical neurons. Trends Neurosci 13:99–104.

Crair MC, Malenka RC (1995) A critical period for long-term potentiation at thalamocortical synapses. Nature 375:325–328.

Cull-Candy S, Brickley S, Ferrant M (2001) NMDA receptor subunits: diversity, development and disease. Curr Opin Neurobiol 11:327–335.

Cynader M, Mitchell DE (1980) Prolonged sensitivity to monocular deprivation in dark-reared cats. J Neurophysiol 43:1026–1040.

Fagiolini M, Pizzorusso T, Berardi N, Domenici L, Maffei L (1994) Functional postnatal development of the rat primary visual cortex and the role of visual experience: dark rearing and monocular deprivation. Vision Res 34:709–720.

Feldman DE (2000) Timing-based LTP and LTD at vertical inputs to layer II/III pyramidal cells in rat barrel cortex. Neuron 27:45–56.

Fischer G, Mutel V, Trube G, Malherbe P, Kew JNC, Mohacsi E, Heitz MP, Kemp JA (1997) Ro 25–6981, a highly potent and selective blocker of *N*-methyl-D-aspartate receptors containing the NR2B subunit. Characterization *in vitro*. J Pharmacol Exp Ther 283:1285–1292.

Flint AC, Maisch US, Weishaupt JH, Kriegstein AR, Monyer H (1997)

NR2A subunit expression shortens NMDA receptor synaptic currents in developing neocortex. J Neurosci 17:2469–2476.
Fox K, Daw NW (1993) Do NMDA receptors have a critical function in visual cortical plasticity? Trends Neurosci 16:116–122.
Frégnac Y, Imbert M (1984) Development of neuronal selectivity in primary visual cortex of cat. Physiol Rev 64:325–434.
Gilbert CD (1998) Adult cortical dynamics. Physiol Rev 78:467–485.
Gordon JA, Cioffi D, Silva AJ, Stryker MP (1996) Deficient plasticity in the primary visual cortex of α-calcium/calmodulin-dependent protein kinase II mutant mice. Neuron 17:491–499.
Hensch TK, Fagiolini M, Mataga N, Stryker MP, Baekkeskov S, Kash SF (1998a) Local GABA circuit control of experience-dependent plasticity in developing visual cortex. Science 282:1504–1508.
Hensch TK, Gordon JA, Brandon EP, McKnight GS, Idzerda RL, Stryker MP (1998b) Comparison of plasticity *in vivo* and *in vitro* in the developing visual cortex of normal and protein kinase A RIβ-deficient mice. J Neurosci 18:2108–2117.
Hestrin S (1992) Developmental regulation of NMDA receptor-mediated synaptic currents at a central synapse. Nature 357:686–689.
Huang ZJ, Kirkwood A, Pizzorusso T, Porciatti V, Morales B, Bear MF, Maffei L, Tonegawa S (1999) BDNF regulates the maturation of inhibition and the critical period of plasticity in mouse visual cortex. Cell 98:739–755.
Husi H, Ward MA, Choudhary JS, Blackstock WP, Grant SGN (2000) Proteomic analysis of NMDA receptor-adhesion protein signaling complexes. Nat Neurosci 3:661–669.
Katz LC, Shatz CJ (1996) Synaptic activity and the construction of cortical circuits. Science 274:1133–1138.
Kimura F, Nishigori A, Shirokawa T, Tsumoto T (1989) Long-term potentiation and *N*-methyl-D-aspartate receptors in the visual cortex of young rats. J Physiol (Lond) 414:125–144.
Kirkwood A, Bear MF (1994) Hebbian synapses in visual cortex. J Neurosci 14:1634–1645.
Kirkwood A, Lee H-K, Bear MF (1995) Co-regulation of long-term potentiation and experience-dependent synaptic plasticity in visual cortex by age and experience. Nature 375:328–331.
Kirkwood A, Silva A, Bear MF (1997) Age-dependent decrease of synaptic plasticity in the neocortex of αCaMKII mutant mice. Proc Natl Acad Sci USA 94:3380–3383.
Komatsu Y (1994) Age-dependent long-term potentiation of inhibitory synaptic transmission in rat visual cortex. J Neurosci 4:6488–6499.
Komatsu Y, Iwakiri M (1993) Long-term modification of inhibitory synaptic transmission in developing visual cortex. NeuroReport 4:907–910.
Komatsu Y, Nakajima S, Toyama K (1991) Induction of long-term potentiation without participation of *N*-methyl-D-aspartate receptors in kitten visual cortex. J Neurophysiol 65:20–32.
Llano I, Leresche N, Marty A (1991) Calcium entry increases the sensitivity of cerebellar Purkinje cells to applied GABA and decreases inhibitory synaptic currents. Neuron 6:565–574.
Lu H-C, Gonzalez E, Crair MC (2001) Barrel cortex critical period plasticity is independent of changes in NMDA receptor subunit composition. Neuron 32:619–634.
Lu YM, Mansuy IM, Kandel ER, Roder J (2000) Calcineurin-mediated LTD of GABAergic inhibition underlies the increased excitability of CA1 neurons associated with LTP. Neuron 26:197–205.
Luo J, Wang Y, Yasuda RP, Dunah AW, Wolfe BB (1997) The majority of *N*-methyl-D-aspartate receptor complexes in adult rat cerebral cortex contain at least three different subunits (Nr1/NR2A/NR2B). Mol Pharmacol 51:79–86.
Maejima T, Ohno-Shosaku T, Kano M (2001) Endogenous cannabinoid as a retrograde messenger from depolarized postsynaptic neurons to presynaptic terminals. Neurosci Res 40:205–210.
Malenka RC, Nicoll RA (1999) Long-term potentiation: A decade of progress? Science 285:1870–1874.
Mason A, Larkman A (1990) Correlation between morphology and electrophysiology of pyramidal neurons in slices of rat visual cortex. II. Electrophysiology. J Neurosci 10:1415–1428.
Monyer H, Burnashev N, Laurie DJ, Sakmann B, Seeburg PH (1994) Developmental and regional expression in the rat brain and functional properties of four NMDA receptors. Neuron 12:529–540.
Mori H, Mishina M (1995) Structure and function of the NMDA receptor channel. Neuropharmacology 34:1219–1237.
Mutel V, Buchy D, Klingelschmidt A, Messer J, Bleuel Z, Kemp JA, Richards JG (1998) In vitro binding properties in rat brain of [^{3}H]Ro 25–6981, a potent and selective antagonist of NMDA receptors containing NR2B subunits. J Neurochem 70:2147–2155.
Nase G, Weishaupt J, Stern P, Singer W, Monyer H (1999) Genetic and epigenetic regulation of NMDA receptor expression in the rat visual cortex. Eur J Neurosci 11:4320–4326.
Philpot BD, Sekhar AK, Shouval HZ, Bear MF (2001) Visual experience and deprivation bidirectionally modify the composition and function of NMDA receptors in visual cortex. Neuron 29:157–169.
Pitler TA, Alger BE (1992) Postsynaptic spike firing reduces synaptic $GABA_A$ responses in hippocampal pyramidal cells. J Neurosci 12:4122–4132.
Quinlan EM, Philpot BD, Huganir RL, Bear MF (1999) Rapid, experience-dependent expression of synaptic NMDA receptors in visual cortex *in vivo*. Nat Neurosci 2:352–357.
Regehr WG, Tank DW (1994) Dendritic calcium dynamics. Curr Opin Neurobiol 4:373–382.
Roberts EB, Ramoa AS (1999) Enhanced NR2A subunit expression and decreased NMDA receptor decay time at the onset of ocular dominance plasticity in the ferret. J Neurophysiol 81:2587–2591.
Seeburg PH (1993) The molecular biology of mammalian glutamate receptor channels. Trends Neurosci 16:359–365.
Sheng M, Cummings J, Roldan LA, Jan YN, Jan LY (1994) Changing subunit composition of heteromeric NMDA receptors during development of rat cortex. Nature 368:144–147.
Shi J, Townsend M, Constantine-Paton M (2000) Activity-dependent induction of tonic calcineurin activity mediates a rapid developmental downregulation of NMDA receptor currents. Neuron 28:103–114.
Singer W (1995) Development and plasticity of cortical processing architectures. Science 270:758–764.
Sprengel R, Suchanek B, Amico C, Brusa R, Burnashev N, Rozov A, Hvalby O, Jensen V, Paulsen O, Andersen P, Kim JJ, Thompson RF, Sun W, Webster LC, Grant SGN, Eilers J, Konnerth A, Li J, McNamara JO, Seeburg PH (1998) Importance of the intracellular domain of NR2 subunits for NMDA receptor function in vivo. Cell 92:279–289.
Stelzer A, Slater NT, Bruggencate GT (1987) Activation of NMDA receptors blocks GABAergic inhibition in an in vitro model of epilepsy. Nature 326:698–701.
Sun XJ, Tolbert LP, Hildebrand JG, Meinertzhagen IA (1998) A rapid method for combined laser scanning confocal microscopic and electron microscopic visualization of biocytin or neurobiotin-labeled neurons. J Histochem Cytochem 46:263–273.
Thomson AM, Deuchars J (1994) Temporal and spatial properties of local circuits in neocortex. Trends Neurosci 17:119–126.
Tovar KR, Westbrook GL (1999) The incorporation of NMDA receptors with a distinct subunit composition at nascent hippocampal synapses *in vitro*. J Neurosci 19:4180–4188.
Trachtenberg JT, Trepel C, Stryker MP (2000) Rapid extragranular plasticity in the absence of thalamocortical plasticity in the developing primary visual cortex. Science 287:2029–2032.
Vicini S, Wang JF, Li JH, Zhu WJ, Wang YH, Luo JH, Wolfe BB, Grayson DR (1998) Functional and pharmacological differences between recombinant *N*-methyl-D-aspartate receptors. J Neurophysiol 79:555–566.
Watanabe M, Inoue Y, Sakimura K, Mishina M (1992) Developmental changes in distribution of NMDA receptor subunit mRNAs. NeuroReport 3:1138–1140.
Wiesel TN (1982) Postnatal development of the visual cortex and the influence of environment. Nature 299:583–592.
Williams K, Russell SL, Shen YM, Molinoff PB (1993) Developmental switch in the expression of NMDA receptors occurs in vivo and in vitro. Neuron 10:267–278.
Yoshimura Y, Tsumoto T (1994) Dependence of LTP induction on postsynaptic depolarization: a perforated patch-clamp study in visual cortical slices of young rats. J Neurophysiol 71:1638–1645.
Yoshimura Y, Sato H, Imamura K, Watanabe Y (2000) Properties of horizontal and vertical inputs to pyramidal cells in the superficial layers of the cat visual cortex. J Neurosci 20:1931–1940.